Parallel Processing in the Corticogeniculate Pathway of the Macaque Monkey

Farran Briggs and **W. Martin Usrey**[*]
Center for Neuroscience and the Departments of Neurobiology, Physiology & Behavior and Neurology, University of California, Davis

Summary

Although corticothalamic feedback is ubiquitous across species and modalities, its role in sensory processing is unclear. This study provides the first detailed description of the visual physiology of corticogeniculate neurons in the primate. Using electrical stimulation to identify corticogeniculate neurons, we distinguish three groups of neurons with response properties that closely resemble those of neurons in the magnocellular, parvocellular and koniocellular layers of their target structure, the lateral geniculate nucleus (LGN) of the thalamus. Our results indicate that corticogeniculate feedback in the primate is stream-specific and provide strong evidence in support of the view that corticothalamic feedback can influence the transmission of sensory information from the thalamus to the cortex in a stream-selective manner.

Keywords

feedback; corticothalamic; V1; LGN; thalamus

Introduction

Few pathways in the nervous system are as prominent, yet poorly understood, as the corticothalamic feedback pathway. Across sensory systems, corticothalamic feedback completes a reciprocal loop of information exchange between the thalamus and cerebral cortex (reviewed in Sherman and Guillery, 2005; Jones, 2007). Such organization provides the cortex with the opportunity to dynamically regulate and shape the nature of its input. Recently, several hypotheses have emerged to describe the function of corticothalamic feedback in sensory processing. These include more generalized roles whereby feedback coordinates activity between the cortex and the thalamus (Bal et al., 2000; Blumenfeld and McCormick, 2000; Destexhe, 2000; Steriade, 2001; Rigas and Castro-Alamancos, 2007), as well as more specialized roles specific to the tuning properties and receptive fields of thalamic neurons (Krupa et al., 1999; Jones et al., 2000; Rivadulla et al., 2002; Webb et al., 2002; Suga and Ma, 2003; Temereanca and Simons, 2004; Cudiero and Sillito, 2006; Li and Ebner, 2007; Nolt et al., 2007). An open and unresolved question is whether or not corticothalamic feedback serves these roles in a manner that is stream-specific. This question is of particular interest given the segregation of feedforward thalamocortical pathways into parallel processing streams. In order

[*]Correspondence: Center for Neuroscience, University of California, Davis, 1544 Newton Court, Davis, CA 95618, 530 754-5468 ph, 530 757-8827 fax, wmusrey@ucdavis.edu.

to determine if corticogeniculate feedback is stream-specific, we studied the physiological properties of identified corticogeniculate neurons in the visual system of the alert macaque monkey.

Parallel processing streams are especially prominent in the primate visual system. Feedforward projections from the lateral geniculate nucleus (LGN) of the thalamus to primary visual cortex (V1) arise from 3 distinct classes of neurons— magnocellular, parvocellular and koniocellular neurons—that differ in their retinal inputs, visual response properties, and projection patterns in V1 (reviewed in Schiller and Logothetis, 1990; Shapley, 1992; Merigan and Maunsell, 1993; Casagrande and Kaas, 1994; Hendry and Reid, 2000; Kaplan, 2004; Callaway, 2005). Anatomical evidence suggests that feedback projections may also be organized in a parallel fashion, as separate populations of corticogeniculate neurons innervate the magno-, parvo- and possibly even the koniocellular layers of the LGN (Lund et al., 1975; Hendrickson et al., 1978; Conley and Raczkowski, 1990; Fitzpatrick et al., 1994; Ichida and Casagrande, 2002; see also Usrey and Fitzpatrick, 1996). However, an examination of the local cortical inputs onto individual neurons in layer 6 of V1—the sole layer to contain corticogeniculate neurons —reveals a diversity of input patterns with some neurons receiving stream-specific input and others receiving mixed input (Briggs and Callaway, 2001). Given the diversity of input patterns to layer 6 neurons, it is difficult to predict whether corticogeniculate neurons are aligned into stream-specific classes, functionally homogeneous, or aligned along some other axis.

Here, we provide the first detailed description of the visual physiology of identified corticogeniculate neurons in any primate species. By recording from corticogeniculate neurons in the alert macaque monkey, we identify 3 classes of neurons with response properties that closely resemble those of neurons in the magnocellular, parvocellular and koniocellular layers of the LGN. These data indicate that corticogeniculate feedback follows the magnocellular/ parvocellular/koniocellular segregation of feedforward projections and provide strong support for the hypothesis that corticothalamic projections exert their influence on the LGN in a stream-specific manner.

Results

Despite the prominence of their projections, corticogeniculate neurons in the macaque monkey constitute a small proportion (<14%; Fitzpatrick et al., 1994) of the physiologically diverse population of layer 6 neurons (Hawken et al., 1988; Ringach et al., 2002). We therefore used a two-step process to identify them physiologically in the alert animal (see Experimental Procedures). First, cortical neurons were identified that faithfully followed electrical stimulation to the LGN via the orthodromic or antidromic propagation of spikes. A collision test was then performed to determine whether the recorded neuron provided feedback projections to the LGN and/or received feedforward input from the LGN (Harvey, 1978; Tsumoto and Suda, 1980; Swadlow and Weyand, 1981, 1987; Grieve and Sillito, 1995; Briggs and Usrey, 2005, 2007). In a collision test, electrical stimulation is triggered by the occurrence of a spontaneous spike in the recorded neuron. If the neuron has an axon that projects to the LGN, then the spontaneous spike traveling toward the LGN will collide with the electrically-evoked antidromic spike and, given the refractory state of the axon, the antidromic spike will not reach the cortex, as in Supplemental Figure 1A. On the other hand, if the cortical neuron receives feedforward input from the LGN, then the spontaneous spike will not affect the propagation of the orthodromic spike and the neuron will faithfully follow the orthodromic spike. These procedures require a close retinotopic register between the stimulating and recording electrodes. Accordingly, we could only antidromically activate corticogeniculate neurons when their receptive fields were within <2° of those at the position of the stimulating electrode.

Response latency and cell classification

There was a broad distribution of antidromic activation latencies across our sample of corticogeniculate neurons with a peak at 4-6 msec and a tail that extended out toward longer latencies (Figure 1A; range: 1.4 – 35.5 msec, mean = 10.3 ± 0.95 msec, n=78 cells). A subset of corticogeniculate neurons, all with short antidromic latencies (<7 msec), also received feedforward suprathreshold input from the LGN (Figure 1A, grey bars, n=10 cells). These values, as well as the shape of the latency distribution, are similar to those recently reported in a study examining the strength of feedforward input onto corticogeniculate neurons in the macaque monkey (Briggs and Usrey, 2007).

Forty corticogeniculate neurons were held for sufficient time to assess their visual response properties. This was accomplished by recording neuronal responses to drifting sinusoidal gratings presented to the receptive fields of neurons while animals fixated on a central spot (see Experimental Procedures for details). Neurons were classified as simple or complex based on the ratio of their first harmonic (f1) to mean (f0) response, where simple cells have an f1 to f0 ratio greater than 1.0 and complex cells have a ratio less than 1.0 (Skottun et al., 1991). A comparison of the f1 to f0 ratio with the antidromic activation latency of neurons revealed a striking segregation of neurons into three groups: complex cells with fast conducting axons (Figure 1B, black diamonds, n = 17); simple cells with medium conducting axons (Figure 1B, red circles, n = 10); and complex cells with slow conducting axons (Figure 1B, blue triangles, n = 13). Differences in the antidromic activation latencies of these 3 groups of cells were highly significant (Figure 1C; fast complex cells = 4.8 ± 0.3 msec, simple cells = 9.7 ± 0.7 msec, slow complex cells = 23.9 ± 2.1 msec; mean $\pm$SEM; $p=4\times10^{-8}$, Kruskal-Wallis test). The subset of corticogeniculate neurons that received suprathreshold, feedforward input from the LGN included only fast complex cells. These cells did not differ from the remaining fast complex cells in their visual physiology and are indicated in Figures 1-5 as unfilled black diamonds.

In the feedforward projections from retina to LGN and LGN to V1, neurons with fast conducting axons generally have shorter visual response latencies than neurons with slower conducting axons (Maunsell et al., 1999; also see Stone, 1983). We therefore examined the visual response latencies of the complex cells in our sample, i.e. those with the fastest and slowest conducting axons (see Supplemental Figure 1B). Simple cells were not included in this analysis, as response latency for this group of cells depends on the starting phase of the stimulus, which differed across cells. Consistent with results from feedforward-projecting neurons, complex cells with fast antidromic latencies displayed significantly shorter visual response latencies than complex cells with slow antidromic latencies (Figures 1D and 1E; visual response latency: fast complex cells = 46.1 ± 1.7 msec, slow complex cells = 68.6 ± 2.5 msec; mean $\pm$SEM; $p=4\times10^{-6}$, Mann-Whitney U-test).

Tuning properties of corticogeniculate neurons

Having identified 3 groups of corticogeniculate neurons on the basis of antidromic latency and the f1 to f0 ratio, we next wished to know whether neurons in these groups also differed from each other with respect to other aspects of their visual physiology, i.e. contrast sensitivity, temporal frequency tuning, size (area summation) tuning, orientation tuning, and direction selectivity.

Past studies have shown that contrast response functions and temporal frequency tuning curves are useful measures for distinguishing different classes of retinal ganglion cells and LGN neurons. In particular, magnocellular LGN neurons respond better than parvocellular neurons to low contrast stimuli and stimuli moving at high temporal frequencies (Kaplan and Shapley, 1986; Kaplan and Benardete, 2001; but see Hawken et al., 1996). Among our sample of corticogeniculate neurons, we also found significant differences in these measures between the

complex cells and simple cells (Figures 2A, 2B and 2E, 2F). Compared to simple cells, both groups of complex cells (fast and slow) displayed a leftward shift in their contrast response functions and a rightward shift in their temporal frequency tuning curves. Accordingly, the contrast required to evoke a half-maximum response (C_{50}) was significantly less for complex cells than simple cells (Figures 2C and 2D; fast complex cells = 13.7 ±1.8% contrast, slow complex cells = 18.4 ±2.1% contrast, simple cells = 37.5 ±4.5% contrast, mean ±SEM; p=6×10^{-6}, Kruskal-Wallis test). Likewise, the highest temporal frequency to evoke a half-maximum response (TF high$_{50}$) was significantly greater for complex cells than simple cells (Figures 2G and 2H; fast complex cells = 25.2 ±2.6 Hz, slow complex cells = 21.8 ±3.3 Hz, simple cells = 9.6 ±1.6 Hz, mean ±SEM; p=0.0012, Kruskal-Wallis test). These results indicate a greater sensitivity among complex cells to stimuli presented at low contrasts and high temporal frequencies. Finally, there was an overall inverse relationship between C_{50} and TF high$_{50}$ across the sample of corticogeniculate neurons (Figure 2I, dashed line) consistent with the notion that neurons responsive to low contrast stimuli are also more responsive to fast moving stimuli.

In addition to the differences in their contrast response functions and temporal frequency tuning curves, simple and complex corticogeniculate neurons also differed from each other in the strength of their surround suppression. Figures 3A and 3B show individual and average area summation tuning curves for the three groups of corticogeniculate neurons (fast complex, simple and slow complex), respectively. These tuning curves were generated from responses to circular spots of drifting, achromatic sine-wave stimuli (presented at 70% contrast, preferred orientation/direction and preferred spatial frequency) that varied in aperture size (diameter). For all three groups of neurons, response rate initially increased as stimulus size increased. Response rate then peaked at a preferred size followed by suppression at larger sizes. Using an area suppression index to quantify the strength of suppression (see Experimental Procedures), we found significantly greater suppression among the two groups of complex cells combined than among the simple cells, i.e. cells with lower f1 to f0 ratios displayed greater area suppression (Figures 3C, dashed line and 3D; area suppression index: complex cells = 0.47 ±0.04, simple cells = 0.28 ±0.05, mean ±SEM; p=0.026, Mann-Whitney U-test). It is worth noting that these suppression index values for the complex and simple corticogeniculate neurons are similar to those reported for magnocellular and parvocellular LGN neurons, respectively (Alitto and Usrey, 2008), providing further support for a relationship between the feedforward and feedback pathways linking the LGN and V1.

Orientation tuning and direction selectivity were useful measures for distinguishing the two groups of complex corticogeniculate neurons—fast and slow (Figure 4A). As shown in Figures 4B and 4C, there was a positive relationship between the antidromic activation latency and orientation tuning bandwidth of corticogeniculate neurons, whereby fast complex cells displayed significantly sharper orientation tuning than slow complex cells (peak half width at half height: fast complex cells = 32.6 ±3.4°, simple cells = 38.3 ±5.5°, slow complex cells = 65.2 ±6.3°, mean ±SEM; p=0.0004, Kruskal-Wallis test). Fast complex cells were also more selective than slow complex cells to the direction of stimulus motion (Figures 4D and 4E; direction selectivity index: fast complex cells = 0.36 ±0.07, simple cells = 0.36 ±0.06, slow complex cells = 0.18 ±0.07, mean ±SEM; p=0.05, Kruskal-Wallis test). Thus, the two groups of complex cells that were initially distinguished by their antidromic activation latencies and visual response latencies are further distinguished by their selectivity to stimulus orientation and direction of motion.

Additional examples of contrast response functions and temporal frequency, area summation and orientation tuning curves from individual neurons representing the three groups of corticogeniculate neurons are provided in Supplemental Figure 2.

Firing rates and cone contributions

Simple and complex corticogeniculate neurons also differed from each other in terms of their maximum firing rates. Although spontaneous activity levels were similar for the three groups of corticogeniculate cells (Figure 5A right; fast complex cells = 19.5 ±3.6 spikes/sec, simple cells = 19.7 ±3.3 spikes/sec, slow complex cells = 18.9 ±4.8 spikes/sec, mean ±SEM), maximum evoked responses were significantly greater among the complex cells than the simple cells (Figure 5A left; fast complex cells = 111.2 ±10.7 spikes/sec, simple cells = 59.1 ±5.8 spikes/sec, slow complex cells = 101.5 ±28.2 spikes/sec; mean ±SEM; p=0.0038, Kruskal-Wallis test). Since magnocellular LGN neurons typically display higher response rates than parvocellular neurons, this result is consistent with the view that there is a relationship between the response properties of neurons in the feedforward and feedback pathways.

To determine the relative contribution of the three cone types—long (L), medium (M) and short (S) wavelength sensitive—to the responses of corticogeniculate neurons, we measured neuronal responses to cone-isolating drifting gratings. Relative cone-contributions were calculated by normalizing neuronal responses to cone-isolating gratings by their responses to contrast-matched, luminance-modulated gratings (see Experimental Procedures). While all three groups of corticogeniculate neurons received strong L- and M-cone input, the slow complex cells received greater S-cone input than either the simple cells or fast complex cells (fast complex cells = 0.6 ±0.2, simple cells = 0.2 ±0.2, slow complex cells = 1.0 ±0.2, mean ±SEM; Figure 5B). Differences in S-cone input were significant for slow complex cells and simple cells (p=0.0075, Kruskal-Wallis test) and near significant for slow and fast complex cells (p=0.12). These results provide evidence for a relationship between slow complex cells and the S-cone dominated koniocellular stream.

Cluster analysis

All of the comparisons made between the response properties of corticogeniculate neuron described thus far have focused on corticogeniculate neurons grouped according to their antidromic latency and f1 to f0 ratio (i.e. fast complex, simple and slow complex cells). We therefore wished to perform an independent analysis on the data where all of the measured responses were weighted equally without any constraints placed on the number of groups or their arrangement within the sample. Figure 6 shows results from a cluster analysis (Matlab, Mathworks Inc.) using six independent and equally weighted parameters: antidromic latency, f1 to f0 ratio, C_{50}, TF high$_{50}$, area suppression index, and direction selectivity index. Only cells held long enough to measure all of these values contributed to this analysis (n = 34 cells). With the exception of a few outliers, this analysis distinguished three major groups of corticogeniculate neurons that match the three groups defined initially on the basis of antidromic latency and the f1 to f0 ratio.

Discussion

Corticogeniculate neurons are in a strategic position to govern the flow of visual information to, from and within V1. Not only do they provide feedback input to the LGN, they also provide local input to the layers of the cortex targeted by LGN axons (Gilbert and Kelly, 1975; Lund et al., 1975; Hendrickson et al., 1978; Fitzpatrick et al., 1994; Wiser and Callaway, 1996; Briggs and Callaway, 2001). Indeed, corticogeniculate neurons are the single greatest source of synaptic input to the LGN and cortical layer 4 (Guillery, 1969; Ahmed et al., 1994, Erisir et al., 1997a,b). Despite the anatomical robustness of their projections, we know little about the functional contributions of corticogeniculate neurons to sensory processing. Moreover, current hypotheses for corticothalamic function have not focused on whether feedback is organized in a stream-specific manner, analogous to the parallel processing channels present in feedforward projections. This study provides the first detailed account of the visual response properties of

identified corticogeniculate neurons in the primate. Using electrical stimulation to identify corticogeniculate neurons in the behaving macaque monkey, we identify three classes of corticogeniculate neurons whose characteristics closely match those of neurons in the magnocellular, parvocellular and koniocellular layers of the LGN. In the sections below, we discuss the relationship between the feedforward and feedback pathways that interconnect the thalamus and visual cortex and consider the broader functional implications of stream-specific feedback.

Feedforward and feedback pathways in the primate visual system

A major hallmark of sensory processing is the separation of feedforward signals into parallel processing streams. Parallel processing serves to increase the operating range and computational abilities of a system as well as to decrease processing time by allowing different components of a stimulus to be analyzed simultaneously. In primates, visual signals leaving the eye are segregated into magnocellular, parvocellular and koniocellular processing streams that remain segregated through the LGN and into V1 (reviewed in Livingstone and Hubel, 1988; Schiller and Logothetis, 1990; Shapley, 1992; Merigan and Maunsell, 1993; Casagrande and Kaas, 1994; Dacey, 2000; Hendry and Reid, 2000; Callaway 2005; Field and Chichilnisky, 2007). In addition to their anatomical segregation, magnocellular, parvocellular and koniocellular stream neurons display distinct physiological properties. By demonstrating physiological segregation of corticogeniculate neurons into magnocellular, parvocellular, and koniocellular-like classes, this study provides strong support for the idea that feedforward and feedback pathways interconnecting the LGN and V1 are organized into similar parallel processing streams.

The response properties of corticogeniculate neurons with fast antidromic activation latencies (<7 msec) and complex cell physiology were extremely similar to those of magnocellular LGN neurons. Both groups of neurons have high contrast gain, follow stimuli at high temporal frequencies, show greater surround suppression, and respond to visual stimuli with shorter latencies and higher firing rates (Schiller and Malpeli, 1978, Kaplan and Shapley, 1982, 1986; Benardete et al., 1992; Maunsell et al., 1999; Usrey and Reid, 2000; White et al., 2001; Solomon et al., 2002; Alitto and Usrey, 2008). Furthermore, fast complex corticogeniculate neurons displayed sharper orientation tuning and greater direction selectivity reminiscent of neurons in layer 4Cα that receive magnocellular input from the LGN (Stone, 1983; Hawken et al., 1988; Merigan and Maunsell, 1993; Gur et al., 2005).

In contrast, corticogeniculate neurons with simple cell response profiles and medium latency axons (7-15 msec) shared many characteristics in common with the parvocellular pathway. Parvocellular stream neurons display less contrast gain, prefer stimuli with lower temporal frequencies and show less surround suppression than magnocellular neurons. Parvocellular stream neurons also have somewhat slower axon conduction latencies and visual response latencies (Schiller and Malpeli, 1978; Bullier and Henry, 1980; Maunsell et al., 1999). Finally, parvocellular-stream neurons receive input almost exclusively from the L- and M-cones in the retina and very little, if any, input from the S-cones (reviewed in De Valois, 2003). Again, we found these exact same traits among our sample of corticogeniculate neurons with simple cell response profiles and medium latency axons.

Complex cells with slow conducting axons form the third group of corticogeniculate neurons identified in this study and these neurons share many features in common with neurons in the feedforward koniocellular stream. Admittedly, much less is known about koniocellular stream neurons compared to those in the magnocellular and parvocellular streams. Still, evidence from bush babies indicates that axon conduction latencies and visual response latencies are slower among koniocellular LGN neurons than magnocellular or parvocellular neurons (Irvin et al., 1986). As a group, koniocellular neurons in the marmoset and bush baby also have contrast

response functions and temporal frequency tuning curves that appear intermediate to those of magnocellular and parvocellular neurons with a bias towards those of magnocellular neurons (Norton et al., 1988; White et al., 1998, 2001; Solomon et al., 1999; Hendry and Reid, 2000; Kaplan, 2004). Perhaps the most notable trait of the koniocellular stream is the prominence of inputs from retinal S-cones (reviewed in Hendry and Reid, 2000; Solomon and Lennie, 2007). Again, all of these traits were found for complex corticogeniculate neurons with slow conducting axons. Finally, while this group of corticogeniculate neurons shares some features in common with the group of fast conducting, complex corticogeniculate neurons (i.e. complex receptive fields, high firing rates), they differ significantly in their orientation tuning and direction selectivity. Taken together, it is rather remarkable how closely the physiology of the three classes of corticogeniculate neurons aligns with the feedforward magnocellular, parvocellular, and koniocellular streams.

The three classes of corticogeniculate neurons distinguished in the current study on the basis of their physiology likely provide anatomically segregated, stream-specific input to the LGN. Past studies using injections of retrograde tracers in the LGN have shown that corticogeniculate neurons in the upper and lower tiers of layer 6 project to distinct layers in the LGN (Lund et al., 1975; Hendrickson et al., 1978; Conley and Raczkowski, 1990; Fitzpatrick et al., 1994; Ichida and Casagrande, 2002; see also Usrey and Fitzpatrick, 1996). In particular, corticogeniculate neurons in the upper tier of layer 6 project to the parvocellular layers of the LGN, while neurons in the lower tier project primarily to the magnocellular layers. Evidence indicates that a small percentage of neurons in the lower tier may also project to the koniocellular layers. With these projection patterns in mind, it is interesting to consider the relative depth of the corticogeniculate neurons that contributed to the current study. Although recording sites could not be reconstructed from lesions in our behaving animals, we often encountered two corticogeniculate neurons in a single electrode penetration and measured their relative positions along the recording track (n = 28 pairs). Among these pairs, we found that simple corticogeniculate neurons were always located above complex corticogeniculate neurons (n = 5 pairs). In addition, the distances separating simple-complex pairs were more than 4 times greater than those separating simple-simple pairs (n = 5) or complex-complex pairs (n = 18; p=0.03, Kruskal-Wallis test). Thus the simple corticogeniculate neurons were most likely located in the upper tier of layer 6 where neurons target the parvocellular layers of the LGN and the complex corticogeniculate neurons were located in the lower tier of layer 6 where neurons target the magnocellular and possibly the koniocellular layers in the LGN.

Interestingly, corticogeniculate neurons retain strong ties to the magnocellular, parvocellular, and koniocellular processing streams, in spite of the fact that V1 contains a myriad of local circuits, many of which mix information from the three input channels (see Merigan and Maunsell, 1993; Callaway, 2004; Sincich and Horton, 2005). Photostimulation experiments measuring local cortical inputs onto layer 6 neurons, including putative corticogeniculate neurons, reveal patterns of stream-specificity in some cells and stream-mixing in others (Briggs and Callaway, 2001). Because corticogeniculate neurons constitute a small proportion of the neurons in layer 6, it seems likely that they are restricted to the population with stream-specific inputs. Additionally, all corticogeniculate neurons in primate V1 have dendrites that allow them the opportunity to sample geniculocortical input directly. Indeed, we have recently shown that corticogeniculate neurons with fast conducting axons and complex physiology receive direct, suprathreshold input from the LGN (Briggs and Usrey, 2007 and Figure 1). Therefore, the magnocellular-like physiological properties displayed by this class of corticogeniculate neurons could be influenced, in part, by direct input from magnocellular LGN neurons. Taken together, both the anatomical and physiological data strongly indicate that corticogeniculate neurons are organized in a stream-specific manner such that feedback can exert selective effects on neurons in the magnocellular, parvocellular and koniocellular layers.

Comparisons with other species and modalities

In the macaque visual system, we see a clear precedent for parallel streams of corticothalamic feedback. This organization begs the question of whether or not parallel streams of feedback are universal across species and sensory modalities. Despite the many differences that exist between species and modalities, existing evidence indicates that parallel streams of feedback may not be unique to the primate or the visual system. For instance, past studies of corticogeniculate neurons in cats, ferrets and rabbits describe multiple cell types based on axonal conduction latency (Harvey, 1978; Tsumoto and Suda, 1980; Swadlow and Weyand, 1987; Briggs and Usrey, 2005). Moreover, some studies distinguish fast and medium latency neurons as having complex and simple receptive fields, respectively (Harvey, 1978; Tsumoto and Suda, 1980; Grieve and Sillito, 1995; Briggs and Usrey, 2005). Thus, the distinction that fast conducting cells are complex and medium conducting cells are simple holds for carnivores and primates. Although other aspects of corticogeniculate physiology have yet to be extensively examined in non-primates, it is tempting to speculate that they also differ along the lines that characterize their respective feedforward pathways (e.g. the Y-, X-, and W-streams).

The distribution of axonal conduction latencies for our sample of corticogeniculate neurons was unimodal with an early peak at short latencies and a tail that extended out toward longer latencies. In contrast, latency distributions for cats, ferrets and rabbits have multiple peaks and troughs that separate the different cell classes (Harvey, 1978; Tsumoto and Suda, 1980; Swadlow and Weyand, 1987; Briggs and Usrey, 2005). Given the smooth shape of the latency distribution in the macaque, it is important to note that the 3 classes of corticogeniculate neurons were distinguished by strict cutoffs in axonal conduction latency (fast complex cells: <7 msec, simple cells: 7-15 msec, slow complex cells: >15 msec).

Similar to the visual system, corticothalamic feedback is robust in the somatosensory and auditory systems. Evidence from the whisker/barrel system of rodents and the auditory system of bats indicates that feedback projections in these systems may also be organized into distinct channels (Ghazanfar et al., 2001; Bokor et al., 2008; Suga, 2008). Thus it appears that evolution has established a precedent for multiple channels of corticothalamic feedback. Future work is still needed in these other systems, however, to determine whether and how these channels of feedback correspond to the feedforward flow of information.

Functional implications

Several roles have been proposed for corticothalamic feedback in sensory processing and these roles generally fall into two main categories (reviewed in Alitto and Usrey, 2003; Briggs and Usrey, 2008). The first category describes feedback as selectively sharpening and/or shifting the receptive fields and tuning functions of thalamic neurons; the other asserts that feedback enhances the transmission of sensory information from receptors to cortex. With respect to the first category, the term "egocentric selection" has emerged which refers to an effect whereby feedback enhances the responses of thalamic neurons with tuning preferences that match those of active corticothalamic neurons and suppresses the activity of thalamic neurons with mismatched tuning (Zhang and Suga, 2000). Evidence in support for egocentric selection comes from studies examining feedback in the auditory system (Suga and Ma, 2003; Wu and Yan, 2007; Zhang and Yan, 2008) and the somatosensory system (Krupa et al., 1999; Ghazanfar et al., 2001; Temereanca and Simons, 2004; Li and Ebner, 2007). In the visual system, corticothalamic feedback and egocentric selection may serve to sharpen the border of the classical receptive field (Murphy and Sillito, 1987; Jones et al., 2000; Rivadulla et al., 2002; Webb et al., 2002; Nolt et al., 2007; but see Bonin et al., 2005; Alitto and Usrey, 2008) and enhance the activity of ensembles of neurons with receptive fields that fall along the orientation axis of their cortical inputs (Wang et al., 2006; Andolina et al., 2007).

The second category of proposed functions for corticothalamic feedback includes several mechanisms for enhancing sensory transmission from the thalamus to the cortex. These include: increasing the gain and reliability of thalamic responses to sensory stimulation (Gulyas et al., 1990; Funke et al., 1996; Cudeiro et al., 2000; Przybyszewski et al., 2000; Wolfart, 2005; Andolina et al., 2007), coordinating membrane states and/or correlated firing patterns between cortical and thalamic network ensembles (Destexhe et al., 1999; Bal et al., 2000; Blumenfeld and McCormick, 2000; Destexhe, 2000; Rigas and Castro-Alamancos, 2007), and mediating the effects of attention and behavior on thalamic activity (Steriade, 2001, 2005; Vanduffel et al., 2000; O'Connor et al., 2002; Monconduit et al., 2006; Wang et al., 2007; McAlonan et al., 2008).

Despite the considerable effort that has been put into elucidating the function(s) of corticothalamic feedback, few studies have examined the issue of whether feedback can influence thalamic activity in a stream-specific manner. Of these, one study reports that feedback selectively increases the responses of parvocellular LGN neurons to stimuli modulated in color in the equiluminant plane (Przbyszewski et al., 2000), and another describes a selective influence of feedback on magnocellular neurons during spatial attention (Vanduffel et al., 2000; but see McAlonan et al., 2008). Given the evidence for parallel channels of corticothalamic feedback, it is important to reexamine corticothalamic function in a stream-specific context. For instance, it will be important to determine whether egocentric selection differs between magnocellular, parvocellular and koniocellular neurons in the LGN and whether correlations in network oscillations and the effects of attention are specific to each processing stream.

Conclusion

In conclusion, we have identified three distinct classes of corticogeniculate neurons in the macaque monkey with physiology characteristic of the magnocellular, parvocellular and koniocellular streams. These results suggest that feedback projections from the cortex to the LGN are stream specific. Furthermore, these findings support the view that corticothalamic neurons preferentially modulated by a particular type of stimulus or behavior can selectively influence information transmission from the thalamus to the cortex in a stream-specific manner.

Experimental Procedures

Two adult male macaque monkeys (*Macacca mulatta*) were used in this study. All procedures conformed to NIH guidelines and were approved by the Institutional Animal Care and Use Committee at the University of California, Davis. Surgical procedures have been described previously (Briggs and Usrey, 2007). Briefly, under full surgical anesthesia, animals were equipped with a scleral eye coil and a cranial implant containing a head restraint post and two recording cylinders located over the LGN and primary visual cortex (V1). Recordings were made from 78 identified corticogeniculate neurons. These neurons had receptive fields at ~4° eccentricity. Data from a subset of these cells (19%) contributed to a recent study examining the strength of feedforward input onto corticogeniculate neurons (Briggs and Usrey, 2007).

Neuronal recordings, electrical stimulation and visual stimulation

Single platinum/iridium stimulating electrodes (FHC, Bowdoin, ME) were semi-chronically implanted within parafoveal regions of the LGN (~4°). The exposed tip of the electrode was < 1 mm and was positioned to excite neurons in both the parvocellular and magnocellular layers. Placement of the stimulating electrode was guided and verified by recording visual responses from the LGN. Stimulating electrodes were connected to an AM systems isolated pulse stimulator (Carlsborg, WA) that delivered a brief, biphasic shock (0.2 msec, ~100mV) in one of two modes: a non-collision mode where shocks were delivered at regular intervals (every 5

seconds), or a collision mode where shocks were triggered to occur within 1 msec of a spontaneous spike from the cortical neuron. Single-unit responses from V1 neurons were made using platinum-in-glass electrodes (Alpha Omega, Israel) and were recorded by a PC equipped with a Power 1401 acquisition system and Spike2 software package (Cambridge Electronic Design, Cambridge, UK).

Corticogeniculate neurons were identified by antidromic activation following LGN stimulation and by a collision test (Briggs and Usrey, 2005, 2007). In a collision test, a spontaneous spike from the recorded cortical neuron triggers the electrical shock. If the cortical neuron is a corticogeniculate neuron that provides feedback to the LGN, then the spontaneous spike traveling toward the LGN will collide with the electrically-evoked antidromic spike and the antidromic spike will not reach the cortex, as in Supplemental Figure 1A. On the other hand, if the cortical neuron receives feedforward input from the LGN, then the spontaneous spike will not affect the propagation of the orthodromic spike and the neuron will produce a spike at the fixed latency. We recorded from a total of 237 V1 neurons that were potentially activated by electrical stimulation in the LGN, of which 78 were confirmed to be corticogeniculate neurons based on offline analyses. Because we used electrical stimulation during our pursuit of corticogeniculate neurons, our sampling procedure was biased toward obtaining corticogeniculate neurons. Thus, our encounter rate does not reflect the actual proportion of corticogeniculate neurons in layer 6 of V1 (33% vs. <14%, Fitzpatrick et al., 1994). Some neurons (10/78) were both antidromically and orthodromically activated by LGN stimulation. In these cases, two spikes (one orthodromic and one antidromic) occurred at fixed latencies during non-collision trials and only one spike (orthodromic) occurred during collision trials.

A number of measures were taken to ensure that corticogeniculate neurons were activated selectively with our stimulation technique. First, stimulating electrodes were implanted in parafoveal regions of the LGN such that the exposed tip (<1 mm) was within the upper and lower margins of the LGN. Second, we used minimal stimulation techniques to ensure that only regions of the LGN local to the electrode tip were activated. Consequently, cortical neurons were only antidromically activated when their receptive fields were within <2° of those at the position of the stimulating electrode. Because electrical stimulation failed to activate corticogeniculate axons at nearby eccentricities in the LGN, it is unlikely that the same stimulation could activate axons outside the LGN. It is also important to note that axons of layer 5 neurons targeting the superior colliculus and pulvinar nucleus travel substantially further from the LGN in the macaque monkey than in carnivores and rodents (Jones, 2007). Finally, antidromically-activated complex cells were never located above simple cells. Because the vast majority of neurons in layer 5 are complex cells (Ringach et al., 2002), we would expect to encounter complex cells above simple cells if we had inadvertently stimulated the axons of layer 5 neurons.

Visual stimuli were generated using a VSG2/5 system (Cambridge Research Systems, Rochester, UK) and presented 700 mm in front of the animal on a gamma-calibrated, Sony monitor (Tokyo, Japan) with a refresh rate of 140 Hz and a mean luminance of 38 cd/m^2. The monitor was the sole source of illumination in the room. All stimuli were presented while animals maintained fixation for a liquid reward. All responses were characterized under binocular viewing conditions. Stimulus presentation began 200 msec following fixation onset. If animals' eye position deviated by >0.35°, trials were aborted. Drifting sinusoidal gratings, centered over the receptive fields of recorded neurons, were used to characterize the visual response properties of recorded neurons. Grating stimuli were shown for 1.4 seconds, followed by 1.4 seconds of mean grey. Following the period of mean grey, the fixation point re-appeared and a new grating was shown. Each stimulus sequence (described below) was generally repeated 3 times. When each stimulus parameter was tested (i.e. contrast, orientation, temporal frequency, spatial frequency, and size), all other parameters were fixed at the optimal setting

for the recorded neuron, with the exception of grating contrast which was fixed at 70%, temporal frequency which was set at 4 Hz, and stimulus size which was ~4 times the size of the receptive field. To generate contrast response functions, gratings of preferred orientation, spatial frequency and temporal frequency were shown over a range of contrasts (0.1%-99.9%) in 16 steps. Orientation tuning and direction selectivity was assessed over the full range of orientations in 24 degree steps. Temporal frequency tuning was assessed over the range of 2 to 32 Hz in 12 steps (4 neurons were tested out to 64 Hz). Area summation was assessed with drifting gratings that varied in aperture size from 0.2 to 10 degrees in 12 steps.

Cone-isolating sinusoidal gratings of varying spatial frequency (0.1 to 3 cycles/degree) were shown at the preferred orientation, direction, and temporal frequency to determine the relative contribution each cone class made to neuronal responses. Cone-isolating gratings were displayed at fixed contrasts: L-cone gratings were 19%, M-cone gratings were 21%, and S-cone gratings were 87% contrast. None of the corticogeniculate neurons in our sample displayed larger responses to cone-isolating gratings compared to luminance-modulated gratings. Therefore, luminance-modulated gratings were used to test orientation, direction, contrast, spatial and temporal frequency and area summation.

Data Analysis and Statistics

Using drifting sinusoidal gratings of optimal orientation, spatial frequency, temporal frequency and 70% contrast, cortical neurons were classified as simple cells or complex cells on the basis of the ratio of the first Fourier coefficient (f1) to mean (f0) response (simple cells: f1/mean > 1.0; complex cells: f1/mean < 1.0; see Skottun et al., 1991). Subsequent analysis of neuronal responses was performed using either the cell's f1 (simple cells) or mean response (complex cells).

To determine the contrast to evoke a half-maximum response (C_{50}), contrast response functions were made from responses to drifting gratings by fitting data to a hyperbolic ratio (Albrecht and Hamilton, 1982),

$$R(C) = K(C^n/(C^n + C_{50}^n)) + DC$$

where C represents the contrast levels presented during the experiment, K represents the maximum response rate, C_{50} is the contrast corresponding to 50% of the cell's maximum response, DC is the firing rate to a blank gray screen, and n is a variable reflecting the cell's sensitivity.

To determine the highest temporal frequency of a stimulus to evoke a half-maximum response (TF high$_{50}$), temporal frequency tuning curves were made from spline-smoothed responses to gratings that varied in temporal frequency (range: 2 – 32 or 64 Hz).

To determine the strength of surround suppression, responses to gratings that differed in aperture size were fitted to a difference-of-Gaussians equation (Sceniak et al., 1999; Alitto et al., 2008),

$$R(S) = R_0 + K_e \int_{-S/2}^{S/2} \exp-(2y/a)^2 * dy - K_i \int_{-S/2}^{S/2} \exp-(2y/b)^2 * dy$$

where S represents aperture size, R_0 represents the spontaneous firing rate, K_e and Ki represent sensitivities to the center and surround, respectively, and a and b represent excitability space

constants. A suppression index (SI) was then used to quantify the amount of suppression using the equation,

$$SI = 1 - (\text{Response}_{(\text{large diameter stimulus})} / \text{Response}_{(\text{preferred diameter stimulus})})$$

To determine orientation tuning and direction selectivity of recorded neurons, responses to gratings that varied in orientation were fitted to a Gaussian equation,

$$R(ori) = K * \exp\left(\frac{-(x - \mu)^2}{2 * \sigma^2}\right) + \text{baseline}$$

where K represents the maximum response rate, x represents the orientations used, μ represents the preferred orientation, σ represents the standard deviation, and baseline is the DC-offset of the Gaussian distribution. Orientation tuning was quantified as peak

half-width at half-height or 1.17σ. Direction selectivity was quantified using a direction index,

$$\text{Direction Index} = \frac{R_1 - R_2}{R_1 + R_2}$$

where R_1 is equal to the response of a neuron to gratings drifting in the preferred direction and R_2 is equal to the response of a neuron to gratings drifting in the opposite direction.

To determine the relative contribution of each cone class to the responses of recorded neurons, we compared neuronal responses to each of the cone-isolating stimuli after normalizing responses to each cell's contrast-matched response to a luminance modulated grating (L-cone contrast = 19%, M-cone contrast = 21%, S-cone contrast = 87%). All comparisons between responses to cone-isolating and luminance modulated gratings were made from gratings shown at the same spatial frequency, which was set to the preferred spatial frequency based on responses to the luminance modulated grating.

Visual response latency was determined for each of the complex cells in the sample based on responses to 6 repeats of a 70% contrast, drifting grating shown at the preferred orientation, spatial frequency, temporal frequency, and size. Visual response latency was defined as the time between stimulus onset (time zero) and half-maximum response (see Supplemental Figure 1B).

For all statistical comparisons, a test for distribution normality (Kolmogorov-Smirnov test) was first performed. For all of the comparisons reported, at least one sample failed the test for normality; therefore non-parametric tests were used for all comparisons (Mann-Whitney U-tests for two-sample comparisons and Kruskal-Wallis tests for multiple-sample comparisons). The cluster analysis was conducted using algorithms pre-programmed in Matlab (Mathworks Inc.). For the cluster analysis, standard Euclidian distances were calculated using the 'pdist' function and the standard shortest-distance metric was used with the 'linkage' function.

Supplementary Material

Refer to Web version on PubMed Central for supplementary material.

Acknowledgments

References

Ahmed B, Anderson JC, Douglas RJ, Martin KA, Nelson JC. Polyneuronal innervation of spiny stellate neurons in cat visual cortex. J Comp Neurol 1994;341:39–49. [PubMed: 8006222]

Albrecht DG, Hamilton DB. Striate cortex of monkey and cat: contrast response function. J Neurophys 1982;48:217–237.

Alitto HJ, Usrey WM. Corticothalamic feedback and sensory processing. Cur Op Neurosci 2003;13:1–6.

Alitto HJ, Usrey WM. Origin and dynamics of extraclassical suppression in the lateral geniculate nucleus of the macaque monkey. Neuron 2008;57:135–146. [PubMed: 18184570]

Andolina IM, Jones HE, Wang W, Sillito AM. Corticothalamic feedback enhances stimulus response precision in the visual system. Proc Natl Acad Sci (USA) 2007;104:1685–1690. [PubMed: 17237220]

Bal T, Debay D, Destexhe A. Cortical feedback controls the frequency and synchrony of oscillations in the visual thalamus. J Neurosci 2000;20:7478–7488. [PubMed: 11007907]

Benardete EA, Kaplan E, Knight BW. Contrast gain control in the primate retina: P cells are not X-like, some M cells are. Vis Neurosci 1992;8:483–486. [PubMed: 1586649]

Blumenfeld H, McCormick DA. Corticothalamic inputs control the pattern of activity generated in thalamocortical networks. J Neurosci 2000;20:5153–5162. [PubMed: 10864972]

Bokor H, Acsady L, Deschenes M. Vibrissal responses of thalamic cells that project to the septal columns of the barrel cortex and to the second somatosensory area. J Neurosci 2008;28:5169–5177. [PubMed: 18480273]

Bonin V, Mante V, Carandini M. The suppressive field of neurons in lateral geniculate nucleus. J Neurosci 2005;25:10844–10856. [PubMed: 16306397]

Briggs F, Usrey WM. Temporal properties of feedforward and feedback pathways between the thalamus and visual cortex in the ferret. Thalamus and Related Systems 2005;3:133–139. [PubMed: 18176624]

Briggs F, Usrey WM. A fast, reciprocal pathway between the lateral geniculate nucleus and visual cortex in the macaque monkey. J Neurosci 2007;27:5431–5436. [PubMed: 17507565]

Briggs F, Usrey WM. Emerging views of corticothalamic function. Cur Op Neurosci. 200810.1016/j.conb.2008.09.002

Bullier J, Henry GH. Ordinal position and afferent input of neurons in monkey striate cortex. J Comp Neurol 1980;193:913–935. [PubMed: 6253535]

Callaway, EM. Cell types and local circuits in primary visual cortex of the macaque monkey. In: Chalupa, LM.; Werner, JS., editors. The Visual Neuroscience. Cambridge, MA: MIT Press; 2004. p. 680-694.

Callaway EM. Structure and function of parallel pathways in the primate early visual system. J Physiol 2005;566:13–19. [PubMed: 15905213]

Casagrande, VA.; Kaas, JH. The afferent, intrinsic, and efferent connections of primary visual cortex in primates. In: Peters, A.; Rockland, KS., editors. Cerebral Cortex Primary Visual Cortex in Primates 10. New York, NY: Plenum Press; 1994. p. 201-259.

Conley M, Raczkowski D. Sublaminar organization within layer VI of the striate cortex in Galago. J Comp Neurol 1990;302:425–436. [PubMed: 1705271]

Cudeiro J, Rivadulla C, Grieve KL. Visual response augmentation in cat (and macaque) LGN: potentiation by corticofugally mediated gain control in the temporal domain. Eur J Neurosci 2000;12:1135–1144. [PubMed: 10762345]

Cudiero J, Sillito AM. Looking back: corticothalamic feedback and early visual processing. Trends Neurosci 2006;29:298–306. [PubMed: 16712965]

Dacey DM. Parallel pathways for spectral coding primate retina. Ann Rev Neurosci 2000;23:743–775. [PubMed: 10845080]

Destexhe A. Modeling corticothalamic feedback and the gating of the thalamus by the cerebral cortex. J Physiol Paris 2000;94:391–410. [PubMed: 11165908]

Destexhe A, Contreras D, Steriade M. Cortically-induced coherence of a thalamic-generated oscillation. Neurosci 1999;92:427–443.

De Valois, RL. Neural coding of color. In: Chalupa, LM.; Werner, JS., editors. The Visual Neurosciences. Cambridge, MA: MIT Press; 2003. p. 1003-1016.

Erisir A, Van Horn SC, Sherman SM. Relative numbers of cortical and brainstem inputs to the lateral geniculate nucleus. Proc Natl Acad Sci (USA) 1997a;94:1517–1520. [PubMed: 9037085]

Erisir A, Van Horn SC, Bickford ME, Sherman SM. Immunocytochemistry and distribution of parabrachial terminals in the lateral geniculate nucleus of the cat: a comparison with corticogeniculate terminals. J Comp Neurol 1997b;377:535–549. [PubMed: 9007191]

Field GD, Chichilnisky EJ. Information processing in the primate retina: circuitry and coding. Ann Rev Neurosci 2007;30:1–30. [PubMed: 17335403]

Fitzpatrick D, Usrey WM, Schofield BR, Einstein G. The sublaminar organization of neurons in layer 6 of macaque striate cortex. Vis Neurosci 1994;11:307–315. [PubMed: 7516176]

Funke K, Nelle E, Li B, Worgotter F. Corticofugal feedback improves the timing of retino-geniculate signal transmission. Neuroreport 1996;7:2130–2134. [PubMed: 8930973]

Ghazanfar AA, Krupa DJ, Nicolelis MAL. Role of cortical feedback in the receptive field structure and nonlinear response properties of somatosensory thalamic neurons. Exp Brain Res 2001;141:88–100. [PubMed: 11685413]

Gilbert CD, Kelly JP. The projections of cells in different layers of the cat's visual cortex. J Comp Neurol 1975;163:81–106. [PubMed: 1159112]

Grieve KL, Sillito AM. Differential properties of cells in the feline primary visual cortex providing the corticofugal feedback to the lateral geniculate nucleus and visual claustrum. J Neurosci 1995;15:4868–4874. [PubMed: 7623117]

Guillery RW. A quantitative study of synaptic interconnections in the dorsal lateral geniculate nucleus of the cat. Z Zellforsch 1969;96:39–48.

Gulyas B, Lagae L, Eysel U, Orban GA. Corticofugal feedback influences the responses of geniculate neurons to moving stimuli. Exp Brain Res 1990;79:441–446. [PubMed: 2323390]

Gur M, Kagan I, Snodderly DM. Orientation and direction selectivity of neurons in V1 of alert monkeys: functional relationships and laminar distributions. Cereb Cortex 2005;15:1207–1221. [PubMed: 15616136]

Harvey AR. Characteristics of corticothalamic neurons in area 17 of the cat. Neurosci Letters 1978;7:177–181.

Hawken MJ, Parker AJ, Lund JS. Laminar organization and contrast sensitivity of direction-selective cells in the striate cortex of the old world monkey. J Neurosci 1988;8:3541–3548. [PubMed: 3193169]

Hawken MJ, Shapley RM, Grosof DH. Temporal-frequency selectivity in monkey visual cortex. Vis Neurosci 1996;13:477–492. [PubMed: 8782375]

Hendrickson AE, Wilson JR, Ogren MP. The neuroanatomical organization of pathways between the dorsal lateral geniculate nucleus and visual cortex in the old world and new world primates. J Comp Neurol 1978;182:123–136. [PubMed: 100530]

Hendry SHC, Reid RC. The koniocellular pathway in primate vision. Ann Rev Neurosci 2000;23:127–153. [PubMed: 10845061]

Ichida JM, Casagrande VA. Organization of the feedback pathway from striate cortex (V1) to the lateral geniculate nucleus (LGN) in the owl monkey (*Aotus trivirgatus*). J Comp Neurol 2002;454:272–283. [PubMed: 12442318]

Irvin GE, Norton TT, Sesma MA, Casagrande VA. W-like response properties of interlaminar zone cells in the lateral geniculate nucleus of a primate (*Galago crassicaudatus*). Brain Res 1986;362:254–270. [PubMed: 3942875]

Jones, EG. The Thalamus. Cambridge, UK: Cambridge University Press; 2007.

Jones HE, Andolina IM, Oakely NM, Murphy PC, Sillito AM. Spatial summation in lateral geniculate nucleus and visual cortex. Exp Brain Res 2000;135:279–284. [PubMed: 11131514]

Kaplan, E. The M, P, and K pathways of the primate visual system. In: Chalupa, LM.; Werner, JS., editors. The Visual Neurosciences 1. Cambridge, MA: MIT Press; 2004. p. 481-493.

Kaplan E, Benardete E. The dynamics of primate retinal ganglion cells. Prog Brain Res 2001;134:17–34. [PubMed: 11702542]

Kaplan E, Shapley RM. X and Y cells in the lateral geniculate nucleus of macaque monkeys. J Physiol 1982;330:125–43. [PubMed: 7175738]

Kaplan E, Shapley RM. The primate retina contains two types of ganglion cells, with high and low contrast sensitivity. Proc Natl Acad Sci (USA) 1986;83:2755–2757. [PubMed: 3458235]

Krupa DJ, Ghazanfar AA, Nicolelis MA. Immediate thalamic sensory plasticity depends on corticothalamic feedback. Proc Natl Acad Sci (USA) 1999;96:8200–8205. [PubMed: 10393972]

Li L, Ebner FF. Cortical modulation of spatial and angular tuning maps in the rat thalamus. J Neurosci 2007;27:167–179. [PubMed: 17202484]

Livingstone MS, Hubel DH. Segregation of form, color, movement, and depth: anatomy, physiology, and perception. Science 1988;240:740–749. [PubMed: 3283936]

Lund JS, Lund RD, Hendrickson AE, Bunt AH, Fuchs AF. The origin of efferent pathways from the primary visual cortex, area 17, of the macaque monkey. J Comp Neurol 1975;164:287–304. [PubMed: 810501]

Maunsell JH, Ghose GM, Assad JA, McAdams CJ, Boudreau CE, Noerager BD. Visual response latencies of magnocellular and parvocellular LGN neurons in macaque monkeys. Vis Neurosci 1999;16:1–14. [PubMed: 10022474]

McAlonan K, Cavanaugh J, Wurtz RH. Guarding the gateway to cortex with attention in visual thalamus. Nature. 200810.1038/nature0738202Epub ahead of print

Merigan WH, Maunsell JH. How parallel are the primate visual pathways? Ann Rev Neurosci 1993;16:369–402. [PubMed: 8460898]

Monconduit L, Lopez-Avila A, Molat JL, Chalus M, Villanueva L. Corticofugal output from the primary somatosensory cortex selectively modulates innocuous and noxious inputs in the rat spinothalamic system. J Neurosci 2006;26:8441–8450. [PubMed: 16914669]

Murphy PC, Sillito AM. Corticofugal feedback influences the generation of length tuning in the visual pathway. Nature 1987;329:727–729. [PubMed: 3670375]

Nolt MJ, Kumbhani RD, Palmer LA. Suppression at high spatial frequencies in the lateral geniculate nucleus of the cat. J Neurophysiol 2007;98:1167–1180. [PubMed: 17596414]

Norton TT, Casagrande VA, Irvin GE, Sesma MA, Petry HM. Contrast-sensitivity functions of W-, X- and Y-like relay cells in the lateral geniculate nucleus of bush baby, *Galago crassicaudatus*. J Neurophys 1988;47:715–741.

O'Connor DH, Fukui MM, Pinsk MA, Kastner S. Attention modulates responses in the human lateral geniculate nucleus. Nat Neurosci 2002;5:1203–1209. [PubMed: 12379861]

Przybyszewski AW, Gaska JP, Foote W, Pollen DA. Striate cortex increases contrast gain of macaque LGN neurons. Vis Neurosci 2000;17:485–494. [PubMed: 11016570]

Rigas P, Castro-Alamancos MA. Thalamocortical Up states: differential effects of intrinsic and extrinsic cortical inputs on persistent activity. J Neurosci 2007;27:4261–4272. [PubMed: 17442810]

Ringach D, Shapley RM, Hawken MJ. Orienation selectivity in macaque V1: diversity and laminar dependence. J Neurosci 2002;22:5639–5651. [PubMed: 12097515]

Rivadulla C, Martinez LM, Valera C, Cudiero J. Completing the corticofugal loop: a visual role for the corticogeniculate type 1 metabotropic glutamate receptor. J Neurosci 2002;22:2956–2962. [PubMed: 11923460]

Sceniak MP, Ringach DL, Hawken MJ, Shapley RM. Contrast's effect on spatial summation by macaque V1 neurons. Nat Neurosci 1999;2:733–739. [PubMed: 10412063]

Schiller PH, Logothetis NK. The color-opponent and broad-band channels of the primate visual system. Trends Neurosci 1990;13:392–398. [PubMed: 1700509]

Schiller PH, Malpeli JG. Functional specificity of lateral geniculate nucleus laminae of the rhesus monkey. J Neurophysiol 1978;41:788–797. [PubMed: 96227]

Shapley, RM. Parallel retinocortical channels: X and Y and P and M. In: Brannan, J., editor. Applications of Parallel Processing in Vision. New York, NY: Elsevier Science Publishers; 1992. p. 3-36.

Sherman, SM.; Guillery, RW. Exploring the thalamus and its role in cortical function. Vol. 2nd. Cambridge, MA: MIT Press; 2005.

Sincich LC, Horton JC. The circuitry of V1 and V2: integration of color, form, and motion. Ann Rev Neurosci 2005;28:303–326. [PubMed: 16022598]

Skottun BC, De Valois RL, Grosof DH, Movshon JA, Albrecht DG, Bonds AB. Classifying simple and complex cells on the basis of response modulation. Vision Res 1991;31:1079–1086. [PubMed: 1909826]

Solomon SG, Lennie P. The machinery of colour vision. Nat Rev Neurosci 2007;8:276–286. [PubMed: 17375040]

Solomon SG, White AJR, Martin PR. Temporal contrast sensitivity in the lateral geniculate nucleus of a new world monkey, the marmoset *Callithrix jacchus*. J Physiol 1999;517:907–917. [PubMed: 10358129]

Solomon SG, White AJ, Martin PR. Extraclassical receptive field properties of parvocellular, magnocellular, and koniocellular cells in the primate lateral geniculate nucleus. J Neurosci 2002;22:338–349. [PubMed: 11756517]

Steriade M. Impact of network activities on neuronal properties in corticothalamic systems. J Neurophys 2001;86:1–39.

Steriade M. Sleep, epilepsy, and thalamic reticular inhibitory neurons. Trends Neurosci 2005;28:317–324. [PubMed: 15927688]

Stone, J. Parallel processing in the visual system. New York, NY: Plenum Press; 1983.

Suga N. Role of corticofugal feedback in hearing. J Comp Physiol A Neuroethol Sens Neural Behav Physiol 2008;194:169–83. [PubMed: 18228080]

Suga N, Ma X. Multiparametric corticofugal modulation and plasticity in the auditory system. Nat Rev Neurosci 2003;4:783–794. [PubMed: 14523378]

Swadlow HA, Weyand TG. Efferent systems of the rabbit visual cortex: laminar distribution of the cells of origin, axonal conduction velocities, and identification of axonal branches. J Comp Neurol 1981;203:799–822. [PubMed: 6173404]

Swadlow HA, Weyand TG. Corticogeniculate neurons, corticotectal neurons, and suspected interneurons in visual cortex of awake rabbits: receptive-field properties, axonal properties, and effects of EEG arousal. J Neurophys 1987;57:977–1001.

Temereanca S, Simons DJ. Functional topography of corticothalamic feedback enhances thalamic spatial response tuning in the somatosensory whisker/barrel system. Neuron 2004;41:639–651. [PubMed: 14980211]

Tsumoto T, Suda K. Three groups of cortico-geniculate neurons and their distribution in binocular and monocular segments of cat striate cortex. J Comp Neurol 1980;193:223–236. [PubMed: 7430428]

Usrey WM, Fitzpatrick D. Specificity in the axonal connections of layer VI neurons in tree shrew striate cortex: evidence for separate granular and supragranular systems. J Neurosci 1996;16:1203–1218. [PubMed: 8558249]

Usrey WM, Reid RC. Visual Physiology of the Lateral Geniculate Nucleus in Two New World Monkeys: *Saimiri sciureus* and *Aotus trivirgatis*. J Physiol 2000;523:755–769. [PubMed: 10718753]

Vanduffel W, Tootell RB, Orban GA. Attention-dependent suppression of metabolic activity in the early stages of the macaque visual system. Cereb Cortex 2000;10:109–126. [PubMed: 10667980]

Wang JY, Chang JY, Woodward DJ, Baccala LA, Han JS, Luo F. Corticofugal influences on thalamic neurons during nociceptive transmission in awake rats. Synapse 2007;61:335–342. [PubMed: 17318884]

Wang W, Jones HE, Andolina IM, Salt TE, Sillito AM. Functional alignment of feedback effects from visual cortex to thalamus. Nat Neurosci 2006;9:1330–1336. [PubMed: 16980966]

Webb BS, Tinsley CJ, Barraclough NE, Easton A, Parker A, Derrington AM. Feedback from V1 and inhibition from beyond the classical receptive field modulates the responses of neurons in the primate lateral geniculate nucleus. Vis Neurosci 2002;19:583–592. [PubMed: 12507325]

White AJR, Solomon SG, Martin PR. Spatial properties of koniocellular cells in the lateral geniculate nucleus of the marmoset *Callithrix jacchus*. J Physiol 2001;533:519–535. [PubMed: 11389209]

White AJR, Wilder HD, Goodchild AK, Sefton AJ, Martin PR. Segregation of receptive field properties in the lateral geniculate nucleus of a new-world monkey, the marmoset *Callithrix jacchus*. J Neurophys 1998;80:2063–2076.

Wiser AK, Callaway EM. Contributions of individual layer 6 pyramidal neurons to local circuitry in macaque primary visual cortex. J Neurosci 1996;16:2724–2739. [PubMed: 8786448]

Wolfart J, Debay D, Le Masson G, Destexhe A, Bal T. Synaptic background activity controls spike transfer from thalamus to cortex. Nat Neurosci 2005;8:1760–1767. [PubMed: 16261132]

Wu Y, Yan J. Modulation of the receptive fields of midbrain neurons elicited by thalamic electrical stimulation through corticofugal feedback. J Neurosci 2007;27:10651–10658. [PubMed: 17913899]

Zhang Y, Suga N. Modulation of responses and frequency tuning of thalamic and collicular neurons by cortical activation in mustached bats. J Neurophysiol 2000;84:325–333. [PubMed: 10899207]

Zhang Y, Yan Y. Corticothalamic feedback for sound-specific plasticity of auditory thalamic neurons elicited by tones paired with basal forebrain stimulation. Cereb Cortex. 2008Epub ahead of print, PMID 18203697
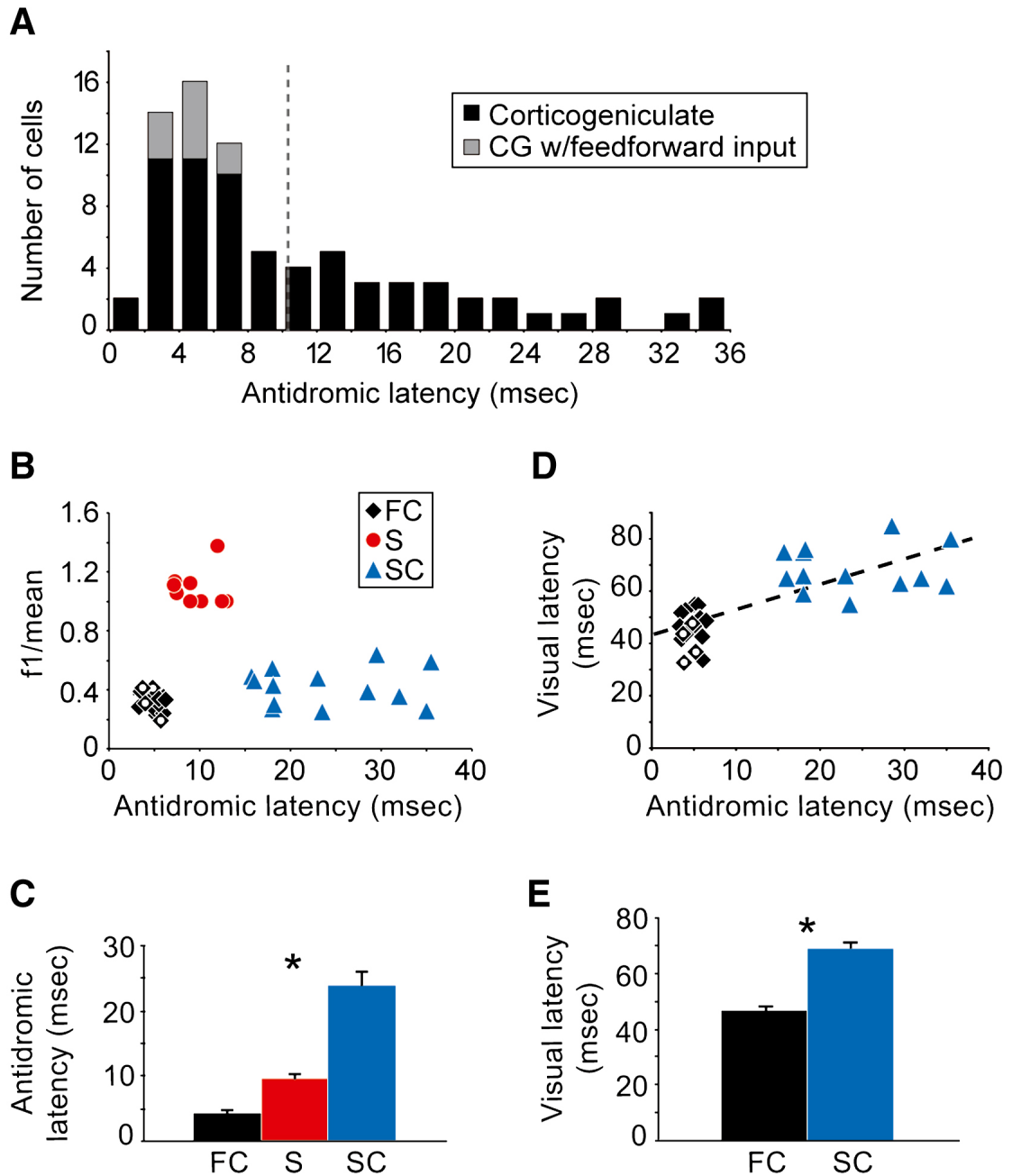
Figure 1. Antidromic response latency and classification of corticogeniculate neurons
(A) Distribution of antidromic response latencies for 78 corticogeniculate neurons. Ten of 78 corticogeniculate neurons also received direct suprathreshold geniculocortical input (indicated by grey bars). Dashed line indicates the mean antidromic latency (10.3 ± 0.95 msec). (B) f1 to f0 ratio versus antidromic latency for 40 corticogeniculate neurons: 17 fast complex cells (FC, black diamonds), 10 simple cells (S, red circles), and 13 slow complex cells (SC, blue triangles). Four corticogeniculate neurons (all FC cells) that also received direct geniculocortical input are indicated by unfilled black diamonds. f1 to f0 values for complex corticogeniculate neurons (FC and SC cells) are significantly lower than those for simple corticogeniculate neurons (S cells; $p=5\times10^{-6}$, Kruskal-Wallis test). (C) Average antidromic latencies of the fast complex

(FC), simple (S) and slow complex (SC) cells. Error bars represent SEM. Asterisk indicates that all three classes of corticogeniculate neurons are significantly different from each other in terms of antidromic latency ($p=4\times10^{-8}$, Kruskal-Wallis test). (D) Visual response latency versus antidromic latency for 17 fast complex cells (FC, black diamonds; corticogeniculate neurons with feedforward input indicated by unfilled diamonds) and 13 slow complex cells (SC, blue triangles). Dashed black line illustrates the linear regression fit to the data ($R^2 = 0.53$, $p=1\times10^{-6}$). (E) Average visual response latencies of fast complex (FC) and slow complex (SC) cells. Error bars represent SEM. Asterisk indicates that the fast complex and slow complex visual response latencies are significantly different ($p=4\times10^{-6}$, Mann-Whitney U-test).
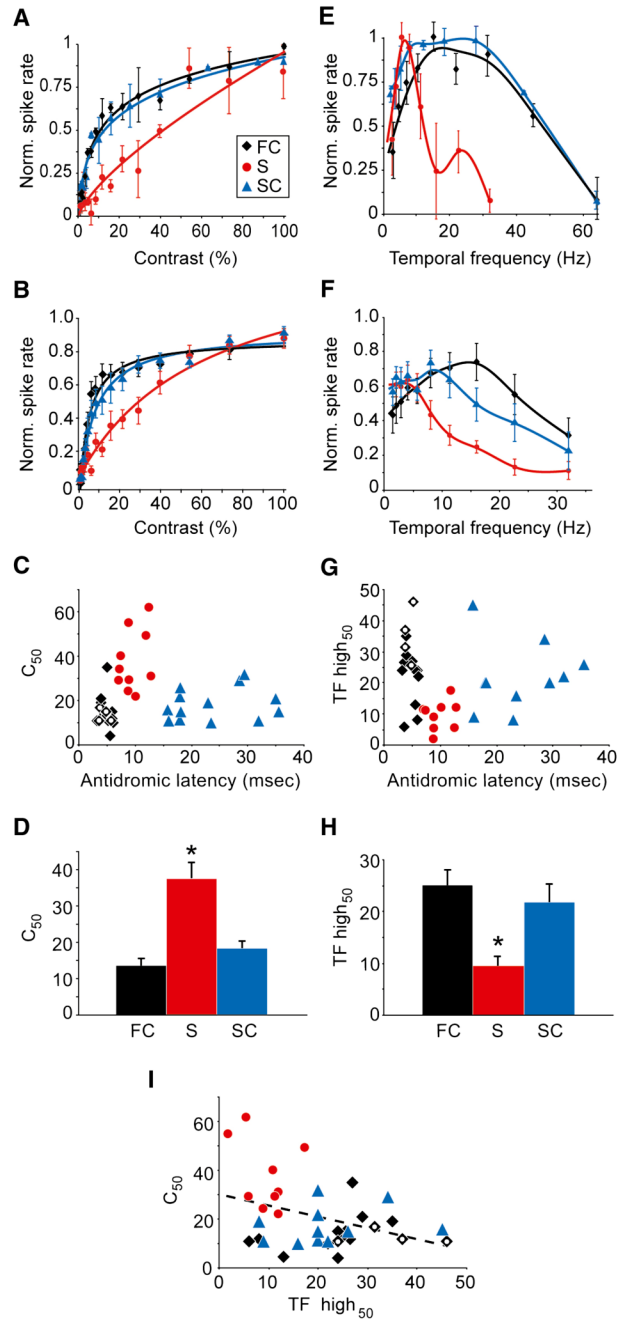
Figure 2. Contrast response functions and temporal frequency tuning curves
(A) Contrast response functions for three corticogeniculate neurons: a fast complex cell (FC, black diamonds), a simple cell (S, red circles), and a slow complex cell (SC, blue triangles). Data were normalized to peaks and fitted with hyperbolic ratio functions. Error bars represent SEM. (B) Average, normalized contrast response functions for all fast complex (17), simple (10), and slow complex cells (13; conventions as in A). (C) C_{50} versus antidromic latency for all fast complex, simple, and slow complex cells. Corticogeniculate neurons (all FC cells) that also received feedforward geniculocortical input indicated by unfilled diamonds. (D) Average C_{50} responses for fast complex (FC), simple (S) and slow complex (SC) cells. Error bars represent SEM. Asterisk indicates that C_{50} values for simple cells are significantly greater than

those of fast complex and slow complex cells (p=6×10^{-6}, Kruskal-Wallis test). (E) Temporal frequency tuning curves for three corticogeniculate neurons: a fast complex, a simple, and a slow complex cell (conventions as in A). Data were normalized to peaks and fitted with smoothing spline functions. Error bars represent SEM. (F) Average, normalized, spline-smoothed temporal frequency tuning curves for 16 fast complex, 9 simple, and 11 slow complex cells (conventions as in E). (G) Comparison of the highest temporal frequencies to evoke a half-maximum response (TF high$_{50}$) versus antidromic latency for fast complex, simple, and slow complex cells (conventions as in C). (H) Average TF high$_{50}$ levels for fast complex (FC), simple (S) and slow complex (SC) cells. Error bars represent SEM. Asterisk indicates that TF high$_{50}$ values for simple cells are significantly lower than those for fast complex and slow complex cells (p=0.0012, Kruskal-Wallis test). (I) C$_{50}$ versus TF high$_{50}$ for fast complex, simple and slow complex cells (conventions as in C and G). Dashed line illustrates the linear regression fit to the data (R^{2} = 0.16, p=0.017).
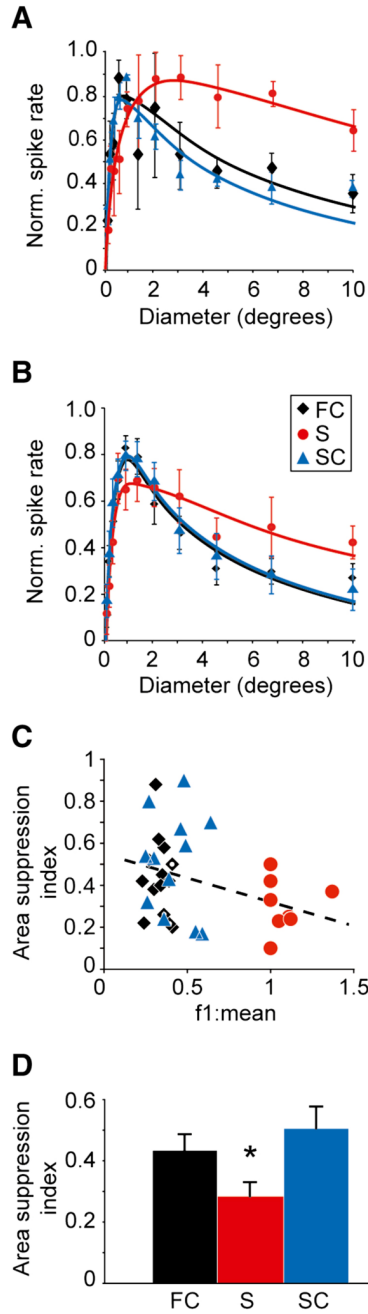
Figure 3. Extra-classical suppression

(A) Individual area summation tuning curves for three corticogeniculate neurons: a fast complex cell (FC, black diamonds), a simple cell (S, red circles), and a slow complex cell (SC, blue triangles). Data were normalized to peaks and fitted with difference of Gaussian functions. Error bars represent SEM. (B) Average, normalized area summation tuning curves for 14 fast complex cells, 9 simple cells, and 12 slow complex cells fitted with difference of Gaussian functions (conventions as in A). (C) Area suppression index values versus f1 to f0 ratios for fast complex, simple, and slow complex cells (conventions as in A; corticogeniculate neurons receiving feedforward geniculocortical input indicated by unfilled diamonds). Dashed line illustrates the linear regression fit to the data ($R^2 = 0.11$, p=0.05). (D) Average area suppression

index values for fast complex (FC), simple (S) and slow complex (SC) cells. Error bars represent SEM. Asterisk indicates that simple cells (S) display less extra-classical suppression than complex cells (FC and SC combined; p=0.026, Mann-Whitney U-test).
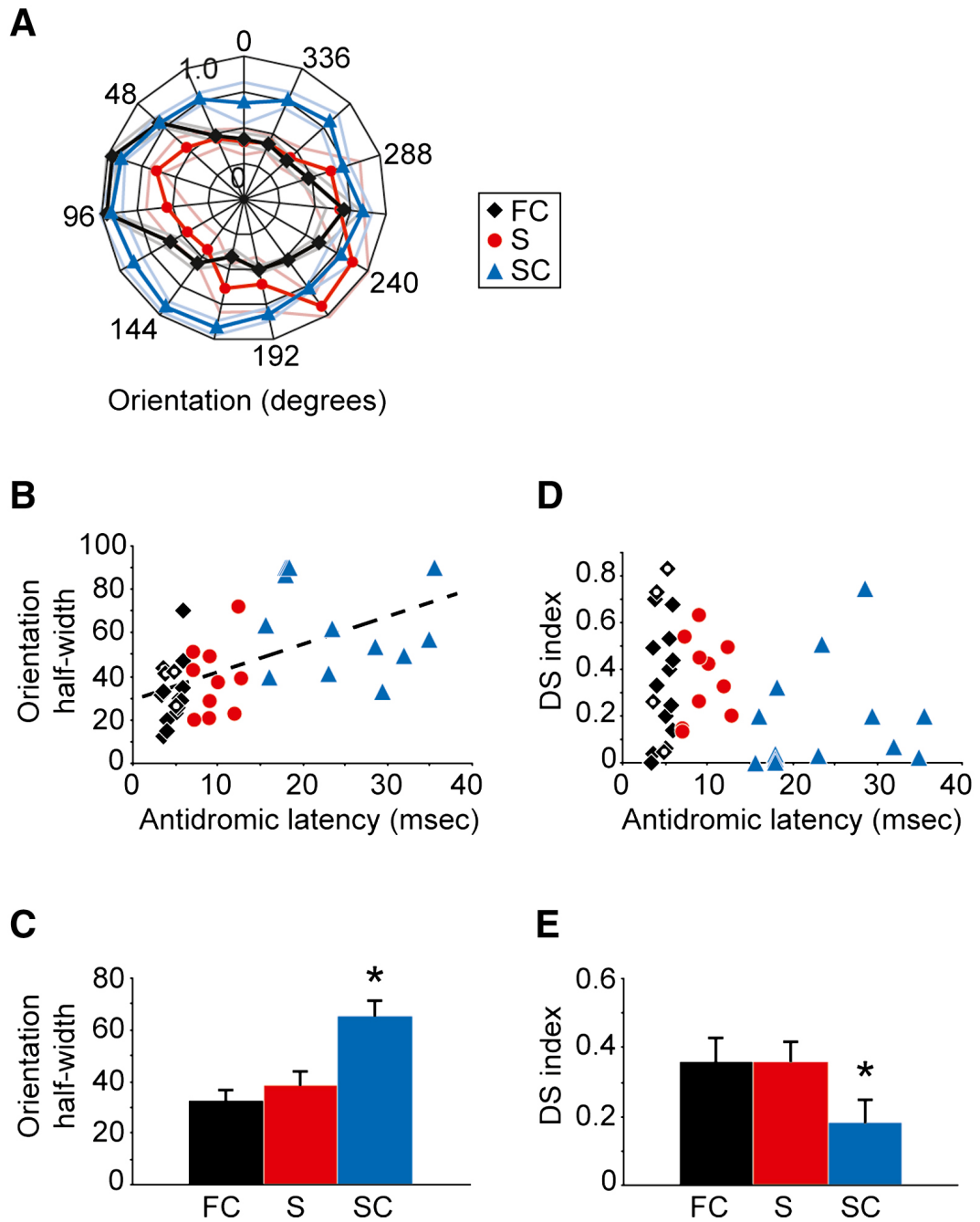
Figure 4. Orientation tuning and direction selectivity
(A) Individual orientation tuning curves for three corticogeniculate neurons: a fast complex (FC, black diamonds), a simple (S, red circles), and a slow complex cell (SC, blue triangles). Data were normalized and plotted in polar coordinates such that the radial axis ranges from 0 to 1.0 normalized spike rate. Lightened lines represent SEM. (B) Orientation tuning bandwidth (peak half-width at half-maximum response) versus antidromic latency for 17 fast complex, 10 simple, and 13 slow complex cells. Corticogeniculate neurons (4 FC cells) that also received feedforward geniculocortical input are indicated by unfilled diamonds. Dashed line illustrates the linear regression fit to the data ($R^2 = 0.36$, $p=4\times10^{-5}$). (C) Average orientation tuning bandwidth values (half-width at half-maximum response) for fast complex (FC), simple (S),

and slow complex (SC) cells. Error bars represent SEM. Asterisk indicates that slow complex cells have significantly larger bandwidth values than fast complex and simple cells (p=0.0004, Kruskal-Wallis test). (D) Direction selectivity index versus antidromic latency for the fast complex, simple, and slow complex cells (conventions as in B). (E) Average direction selectivity index values for fast complex, simple and slow complex cells. Error bars represent SEM. Asterisk indicates that slow complex cells have significantly lower direction selectivity index values than fast complex and simple cells (p=0.05, Kruskal-Wallis test).
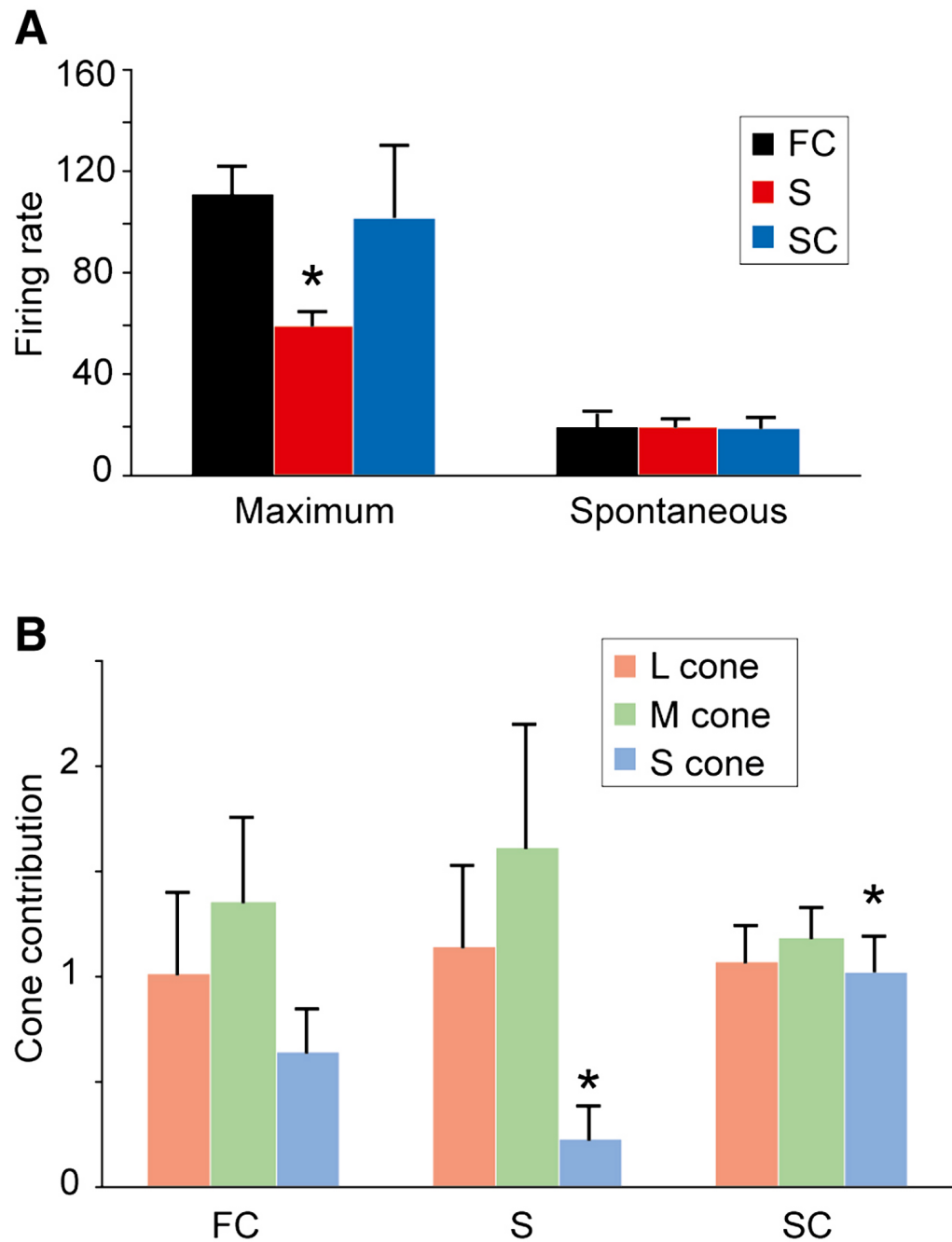
Figure 5. Firing rates and cone-contributions

(A) Average maximum and spontaneous firing rates for 17 fast complex cells (FC, black), 10 simple cells (S, red), and 13 slow complex cells (SC, blue). Error bars represent SEM. Asterisk indicates that simple cells have significantly lower maximum firing rates than fast and slow complex cells (p=0.0038, Kruskal-Wallis test). (B) Average L-cone (light red), M-cone (light green), and S-cone (light blue) contributions to the responses of 8 fast complex cells (FC), 8 simple cells (S) and 10 slow complex cells (SC). Error bars represent SEM. Left asterisk indicates that S-cones contribute significantly less to simple cell responses than L- and M-cones (p=0.027, Kruskal-Wallis test). Right asterisk indicates that slow complex cells receive significantly more S-cone input than simple cells (p=0.0075, Kruskal-Wallis test).
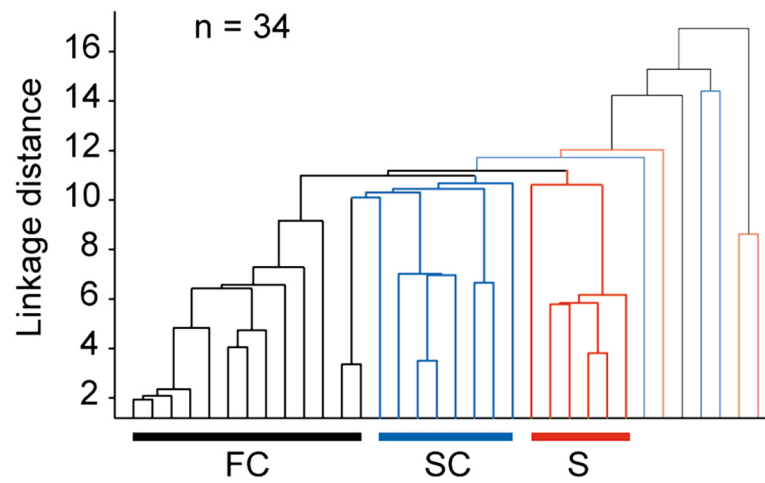
Figure 6. Cluster analysis
Dendrogram for a cluster analysis illustrating linkage distances across 34 corticogeniculate neurons based on 6 response parameters (antidromic latency, f1/mean, C_{50}, TF high$_{50}$, area suppression, and direction selectivity). Fast complex cells (FC) are indicated by black lines and mostly cluster to the left (n = 14), simple cells (S) are indicated by red lines and cluster to the right (n = 9), and slow complex cells (SC) are indicated by blue lines and cluster toward the middle (n = 11).